



Non-Bronchoscopic Assessment of the Airways

13

Alister J. Bates, Nara S. Higano,
and Jason C. Woods

Overview

Bronchoscopy is the current gold standard for assessing structure, function, anomalies, and secretions related to the central airways [1]. However, bronchoscopic evaluations have some important limitations, particularly in the pediatric population. They are invasive and are typically performed under sedation; both of these factors may alter the behavior of the airway from its natural condition. Furthermore, findings can differ between rigid and flexible endoscopes, and there is continued debate over inter-operator agreement in airway assessment, for example, in deter-

mining the presence or absence of tracheomalacia in neonates [2]. These limitations have led to the development of alternative central airway assessment techniques.

Current clinical non-bronchoscopic assessment of the central airways is usually performed through radiological evaluation. Several different imaging modalities are used, including radiography, computed tomography (CT), and magnetic resonance imaging (MRI). The first of these provides a projection of the airway, and the latter two can provide 3D image volumes of the airway and surrounding structures. However, these methodologies have limitations in that they may not represent the air-

A. J. Bates (✉)

Division of Pulmonary Medicine, Cincinnati
Children's Hospital Medical Center,
Cincinnati, OH, USA

Upper Airway Center, Cincinnati Children's Hospital,
Cincinnati, OH, USA

Center for Pulmonary Imaging Research, Division of
Pulmonary Medicine, Cincinnati Children's Hospital,
Cincinnati, OH, USA

Department of Pediatrics, University of Cincinnati,
Cincinnati, OH, USA

e-mail: Alister.bates@cchmc.org

N. S. Higano

Division of Pulmonary Medicine, Cincinnati
Children's Hospital Medical Center,
Cincinnati, OH, USA

Center for Pulmonary Imaging Research, Division of
Pulmonary Medicine, Cincinnati Children's Hospital,
Cincinnati, OH, USA

e-mail: Nara.higano@cchmc.org

J. C. Woods

Division of Pulmonary Medicine, Cincinnati
Children's Hospital Medical Center,
Cincinnati, OH, USA

Upper Airway Center, Cincinnati Children's Hospital,
Cincinnati, OH, USA

Center for Pulmonary Imaging Research, Division of
Pulmonary Medicine, Cincinnati Children's Hospital,
Cincinnati, OH, USA

Department of Radiology, Cincinnati Children's
Hospital, Cincinnati, OH, USA

Department of Pediatrics, University of Cincinnati,
Cincinnati, OH, USA

Departments of Radiology and Physics,
University of Cincinnati, Cincinnati, OH, USA
e-mail: Jason.woods@cchmc.org

way in natural breathing, due to the breathing maneuver performed while the image was acquired (i.e., breath holds), sedation, and intubation. Imaging also does not usually provide functional information about the airway. [Emerging Techniques](#) Section of this chapter describes novel imaging-based techniques to address these limitations and to provide functional airway information such as the patient's breathing effort via computational fluid dynamics simulations of respiratory airflow.

Current Clinical Medical Imaging

Radiography

Initial airway assessment can be performed with frontal and lateral views of the neck and chest on X-ray radiographs (Fig. 13.1). Radiography exposes patients to very low doses of ionizing radiation, and it is generally considered safe in pediatrics [3, 4]. Radiographs are generally used for detecting the presence of foreign bodies within the airway [5, 6] and can also detect some airway conditions, such as croup [7, 8]. In addition, radiography can be used in the diagnosis of

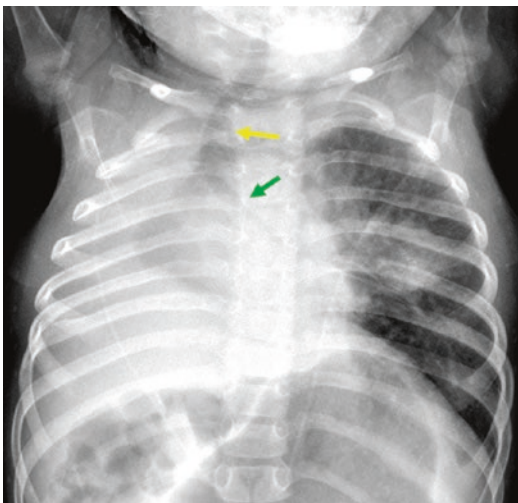


Fig. 13.1 X-ray radiograph. Chest X-ray radiograph in a 2-year-old female patient following a pneumonectomy for a congenital lung lesion. Abnormalities in the central airways are visible, including severe tracheal deviation (yellow arrow) and stenosis in the left main bronchus (green arrow). (Courtesy of Jason Woods, PhD, at Cincinnati Children's Hospital)

laryngomalacia [6], hypertrophy of the adenoids, palatine and lingual tonsils, and the tongue (macroglossia), and airway stenoses. Lateral cephalometry can be performed based on cranial radiographs, but a comparison between these measurements and findings from drug-induced sleep endoscopy (DISE) found little correlation between the methods, with the exception of narrowings in the retroglossal airway [9]. While radiographs may act as a first-line imaging assessment of airway conditions, the information garnered is limited since the single image is a projection of the airway, with little ability to quantify abnormalities or assess dynamics.

Computed Tomography

In current practice, X-ray computed tomography (CT) is considered the gold standard for noninvasive airway assessment [10–12]. Multi-detector CT (MDCT) provides detailed anatomic images with 2D multi-planar or 3D volume renderings. MDCT allows for shortened scan times, allowing for pediatric scans to be performed without the use of sedation or intubation, factors which have historically limited the use of CT for airway diagnostics; sedation can affect the muscle tone of structures surrounding the airways, and intubation can alter anatomical dynamics. The dynamics of the airway during typical breathing or coached inspiratory and expiratory breath-holds can be revealed by repeating MDCT to produce cine, 4D, or inspiratory-expiratory images (Fig. 13.2). However, the dynamic resolution can be limited by the speed of the gantry rotation, and repeated imaging increases the radiation exposure [10–12].

High spatial resolution is often necessary to detect abnormalities in the narrow nasal passages, such as turbinate hypertrophy, septal deviation, and pyriform aperture stenosis. The high-resolution of CT and its ability to produce high contrast between structures such as bone and soft tissue can be used to diagnose a large range of airway abnormalities and the underlying causes [13, 14].

The upper airways can be imaged via CT to determine the effect of surgical interventions to

correct conditions such as Pierre-Robin syndrome. Imaging can be performed preoperatively and postoperatively and the change in lumen size measured, information which may help the decision to decannulate patients [15]. In patients with obstructive sleep apnea (OSA), upper airway CT has been proposed to determine sites of obstruction, to assess surgical interventions, and also as a possible diagnostic alternative to polysomnography [16–18]. At present, while the importance of airway morphology in the severity of OSA is clear, no morphological parameter measured from CT images has been found to separate OSA patients from healthy individuals [19]. A comparison between CT measurements performed in awake patients and DISE classification of the upper airway in adult OSA patients revealed CT-matched DISE in identifying lateral collapse in the oropharynx [20].

In the trachea, CT can be used to diagnose subglottic stenosis and assess the severity of the stenosis [21]. Tracheomalacia (TM) can be analyzed via CT by comparing inspiratory and expiratory images of the airway (Fig. 13.2). The diagnosis of TM is made when the cross-sectional area of the trachea in the expiratory image is >50% less than on inspiration, a criterion originally developed in rigid bronchoscopy [22].

The advantages of CT over other imaging modalities are again the high contrast between the airway and surrounding structures, high spatial resolution, and the ability for 4D imaging. However, the major disadvantage of CT is the patient's exposure to ionizing radiation, and this concern particularly affects its use in pediatrics [23]. While the necessary dose of radiation has been greatly reduced [24, 25], CT is still rarely appropriate for serial imaging to assess changes in the airway as a child develops or to assess the efficacy of treatment strategies. While CT will remain a gold standard, emerging techniques in MRI have been demonstrated to provide images of the respiratory system that are comparable to the spatial and temporal resolution of CT (see Sect. [Developments in Magnetic Resonance Imaging](#)), but without breath-hold maneuvers, sedation/anesthesia, intubation, or ionizing radiation.

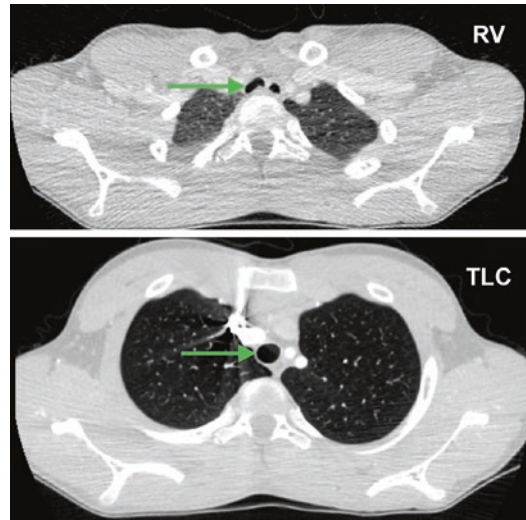


Fig. 13.2 CT of the dynamic trachea. Axial image slices from airway CT in a 14-year-old male with a highly dynamic chest wall. During a forced expiratory maneuver, at residual volume (RV), the trachea (green arrow) narrows significantly due to the narrowing of the chest. Comparison between the expiratory-phase (top) and inspiratory-phase (bottom – at total lung capacity, TLC) images demonstrates dynamic excessive collapse of the posterior tracheal wall. (Courtesy of Alister Bates, PhD, at Cincinnati Children's Hospital)

Magnetic Resonance Imaging

Magnetic resonance imaging provides high contrast between airway and the surrounding soft tissues without exposing the patient to any ionizing radiation. It is therefore suitable for evaluation of treatment through pre- and post-therapy imaging and for serial imaging of patients to monitor growth or disease progression, where multiple radiation exposures via CT would not be appropriate in the pediatric population.

Traditionally, an overall MRI exam consisting of multiple scans has taken 30–60 minutes to perform upper airway analysis [26]. While motion of non-compliant patients is a concern in pediatrics, new techniques such as compressed sensing have accelerated many sequences by up to four times [27]. These emerging techniques have obviated some of the disadvantages of a long acquisition time, through retrospective removal of data obscured by motion (see Sect. [Developments in Magnetic Resonance Imaging](#)) [28].

MRI has been also used clinically as a surgical planning tool for OSA. An MRI exam for OSA may include several scans designed to assess various aspects of a patient's anatomy. Proton density MRI provides a static high-resolution (sub millimeter in-plane resolution) structural image of the airway to highlight narrow points in the airway and the underlying anatomic cause (e.g., macroglossia) (Fig. 13.3) [29]. Cine MRI can provide real-time 2D slices of the airway at high temporal resolutions (e.g., ~3 images per second) to show the motion of the airway and any collapse during an individual breath [29]. Cine MRI is often repeated in several planes such as a midline sagittal plane to reveal anterior-posterior airway collapse, and axial planes at various locations in the airway to assess retropalatal and retroglossal collapse [30–32]. T₂-weighted turbo spin echo imaging can provide contrast in the soft-tissue structures surrounding the airway (e.g., distinguishing the tongue from the lingual tonsils) [29].

Ultrasound

Ultrasound is a fast imaging modality that is tolerated by the majority of pediatric patients, and like MRI, it is considered very safe, as it does not use ionizing radiation. The real-time nature of ultrasound makes it an ideal technique to determine correct positioning and appropriate sizing of an endotracheal tube [33].

Applications of airway ultrasound include assessment of soft-tissue masses in the neck [26]

and guidance for percutaneous tracheostomy [34, 35]. There has been good agreement with endoscopic findings in evaluating vocal cord palsy in children up to 12 years old (81% agreement with endoscopy) [36], in identifying anatomy of subglottic hemangioma [37], and in identifying epiglottitis in patients over 15 years of age [38]. Additionally, ultrasound has been shown to give good agreement with MRI in terms of measuring the minimum airway diameter found in subglottic stenosis [39].

However, a major challenge of airway ultrasound is that air does not propagate the ultrasonic sound waves as effectively as tissues. Thus, it is particularly challenging to image structures surrounded by air, such as the epiglottis and soft palate [33, 40]. As a result, ultrasound has not been widely adopted for airway imaging.

Fluoroscopy

Fluoroscopy provides a continuous X-ray projection through the airway at high temporal resolution for ~10–20 seconds of breathing and has been used to assess motion of the airway in conditions such as OSA, laryngomalacia, or tracheomalacia [31]. A comparison of sleep fluoroscopy to direct laryngoscopy and bronchoscopy to identify upper airway obstruction in 50 pediatric patients found that sleep fluoroscopy identified sites of obstruction not recognized on direct laryngoscopy and bronchoscopy in 54% of cases

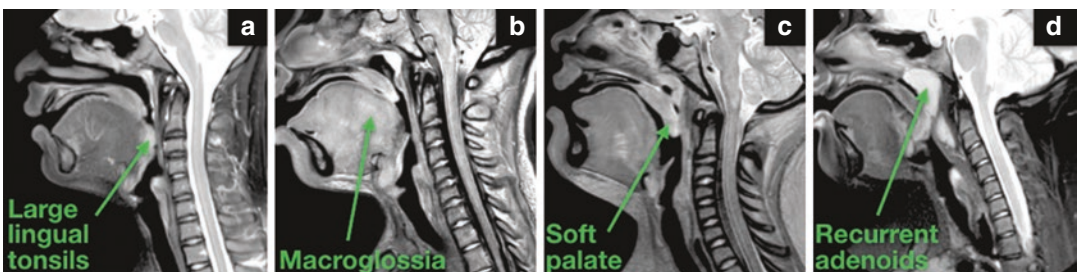


Fig. 13.3 MRI of obstructive sleep apnea. Sagittal static high-resolution MRI of patients with persistent obstructive sleep apnea (OSA) post-adenotonsillectomy. Each panel shows a patient with a specific cause of their OSA, which was identified by MRI. The condition was then

treated with the following procedures: (a) lingual tonsillectomy, (b) partial midline glossectomy, (c) uvulopalatopharyngoplasty, and (d) revision adenoidectomy. (Courtesy of Alister Bates, PhD, at Cincinnati Children's Hospital)

and altered the course of treatment in 52% of cases [41].

In patients who have contraindications for MRI, such as those with hypoglossal nerve stimulators or metallic dental work (which is MR-safe but yields image artifacts), fluoroscopy can be used as an alternative for assessment of airway dynamics. MR-incompatible devices such as nerve stimulators are becoming increasingly popular treatment options for patients with OSA, and fluoroscopy can reveal in-plane airway dynamics post-treatment [42]. However, as fluoroscopy requires cumulative exposure to ionizing radiation, use of a fluoroscope cannot be justified solely by the sensitivity of the test [43], and use of airway fluoroscopy is decreasing in favor of other methods.

Virtual Bronchoscopy

Virtual bronchoscopy is a technique in which the airway structure is digitally recreated from high-resolution 3D images. In current clinical practice, these images are usually generated via CT, although emerging MRI techniques may provide a nonionizing alternative for this technique (see Sect. [Developments in Magnetic Resonance Imaging](#) below). On virtual bronchoscopy, a reader's viewpoint is placed within the airway, in the position where the endoscopic camera lens would be in bronchoscopy (Fig. 13.4). This viewpoint can then be moved along the airway, again as in bronchoscopy. Two techniques exist for displaying the airway: surface rendering and volume render-

ing. In surface rendering, the airway wall surface is digitally recreated where the image transitions from tissue to airway. When based on CT imaging, the transition can often be detected automatically due to the large change in Hounsfield intensity units between air and surrounding tissue. In volume rendering, each voxel in the image is represented in 3D space, with higher-intensity regions of the image (i.e., soft tissue) drawn opaquely and lower-intensity regions (i.e., air in the airway) drawn with more transparency. Therefore, the lumen is completely transparent, and placing the viewpoint inside the lumen reveals the first visible opaque region – the airway wall.

The primary function of virtual bronchoscopy is to present radiologic imaging in a format with which bronchoscopists are familiar. Virtual bronchoscopies can reveal the branching structure of the major airways, stenoses [5, 10], obstructions, and airway abnormalities such as tracheal diverticulum. However, each of these conditions is apparent directly from the radiological images [44–46], and the virtual bronchoscopy is not necessary for diagnosis. Due to virtual bronchoscopy's reliance on the initial imaging, it can only render the behavior of the airway during imaging: dynamic virtual bronchoscopy, comparison of the airway in inspiration and expiration, and breathing maneuvers such as induced coughing can only be performed if images of these behaviors were captured. Virtual bronchoscopy has been compared to flexible bronchoscopy in the diagnosis of pediatric tracheomalacia and was found to be specific, but not sensitive [47].



Fig. 13.4 Invasive and CT-based virtual bronchoscopy. Mild tracheomalacia in the middle and lower trachea of a pediatric patient are observed on both flexible bronchos-

copy (a and b, respectively) and also on virtual bronchoscopy generated from high-resolution computed tomography (CT) images. (From: Su et al. [47])

Emerging Techniques

The ultimate goal of airway analysis is to detect the degree to which airway anatomy and motion affect each patient's ventilation and work of breathing, and how this relationship changes with airway abnormalities. For example, understanding how much a subglottic stenosis increases a patient's work of breathing can inform the clinical recommendation or rapidity of intervention. While current clinical imaging methods can provide useful information on airway abnormalities, they have limitations related to increased patient risks, nonrepresentative breathing conditions, lack of quantitative assessment, and lack of evaluation of airway function. Novel techniques for airway imaging are being developed that address many of the challenges of current methods and may answer questions on airway function in a wide range of airway abnormalities.

Developments in Magnetic Resonance Imaging

Recent imaging developments in MRI have allowed similar capabilities to that of airway CT, without requiring nonionizing radiation. Radial ultrashort echo-time (UTE) MRI is a technique widely used for pulmonary imaging in the research setting. By sampling the rapidly decaying pulmonary MR signal much earlier than conventional MRI (on order of $<100 \mu\text{s}$, compared with $\sim 0.5\text{--}3 \text{ ms}$ depending on magnetic field strength) [48], UTE MRI can yield images with resolution ($\sim 0.7 \text{ mm}$ isotropic) and proton-density image intensity approaching that of CT [49–51]. The time-course of specific UTE MRI raw data also allows the physiologic and bulk motion of the patient during imaging to be assessed retrospectively. Using this information, data acquired while the patient was noncompliantly moving can be discarded and an image created without motion artifact, assuming a reasonable period of quiescent breathing [28]. Furthermore, diaphragm motion can also be detected using similar UTE MRI raw data, allowing retrospective respiratory gating of images from a scan acquired during tidal breathing. Using this technique, high-resolution images show the patient's typical airway

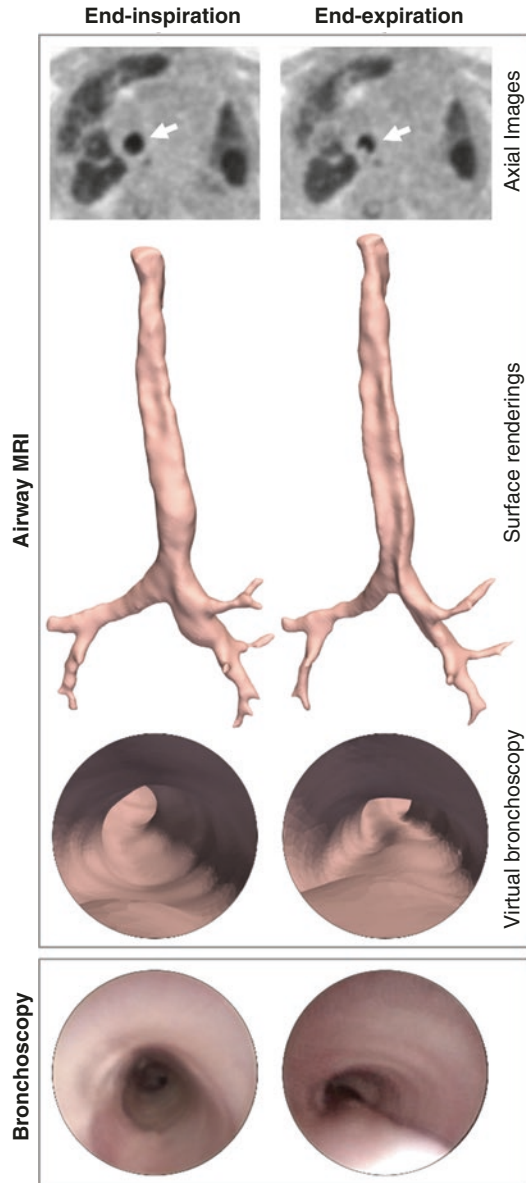


Fig. 13.5 MRI-based virtual bronchoscopy. Severe tracheomalacia in the middle and lower trachea of a male infant with bronchopulmonary dysplasia (BPD) can be observed in the axial slices (top row, arrows), surface renderings (second row), and virtual bronchoscopic views from high-resolution ultrashort echo-time (UTE) MRI, which does not require sedation or ionizing radiation. These MRI-based findings are comparable to those seen on invasive, sedated bronchoscopy (bottom row). (Courtesy of Jason Woods, PhD, Alister Bates, PhD, and Nara Higano, PhD, at Cincinnati Children's Hospital)

structure at several instants throughout the breathing cycle. UTE MRI has been used to quantitatively assess tracheomalacia in neonates with various

respiratory conditions (Fig. 13.5), obtaining good agreement with bronchoscopy [52], and for presur-

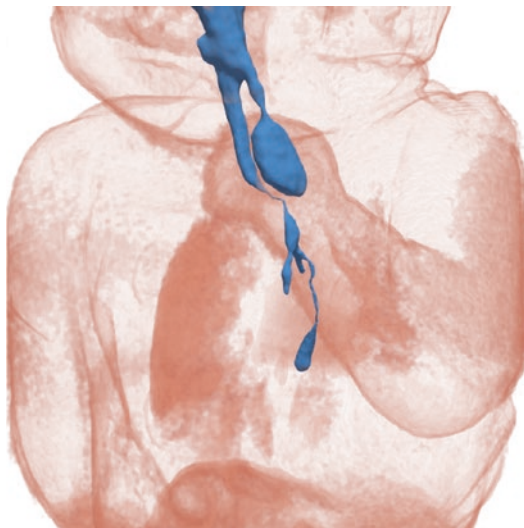


Fig. 13.6 3D anatomical rendering of neonatal congenital tracheoesophageal defects. Oblique left-posterior view of a 3D body volume rendering (red) and a surface rendering of the tracheal and esophageal anatomy (blue) in a female neonatal patient with esophageal atresia/tracheoesophageal fistula. Several anatomical abnormalities are evident: the large proximal esophageal pouch, long narrow fistula between the lower trachea and distal esophageal, and the severely compressed middle trachea. These 3D renderings are generated from high-resolution ultrashort echo-time (UTE) MRI, which does not require sedation or ionizing radiation and offer novel anatomical visualizations that can inform surgical planning decisions prior to operative treatment. (Courtesy of Jason Woods, PhD, Alister Bates, PhD, and Nara Higano, PhD, at Cincinnati Children's Hospital)

gical planning in patients with tracheoesophageal fistulas (Fig. 13.6) [53].

For some conditions, such as OSA, apneic events do not occur every breath, so it is necessary to obtain real-time cine images of the airway dynamics. Real-time cine MRI techniques have been developed to obtain MRI at high temporal resolution (~ten images per second), on a limited number of slices [54]. Other techniques have combined static high-spatial-resolution MRI with high-temporal resolution 4D MRI (~three 3D images per second; Fig. 13.7) to create virtual moving airway surfaces [55, 56].

Geometric Airway Measurements from Imaging

Traditional radiological quantification of airway anatomy has been limited to the measurement of a few key distances, such as the lumen diameter or cross-sectional area in a stenosis. While these values are of value, there is growing recognition that the size and shape of the entire airway influences the airflow within, rather than just a local constriction or in a single imaging slice [57]. Therefore, automatic techniques that measure many aspects of the airway's shape and size along the length of the airway have been developed.

To obtain accurate measurements of the size and the shape of the airway, the airway must be viewed perpendicularly to the lumen cross-section. This orientation can be difficult to

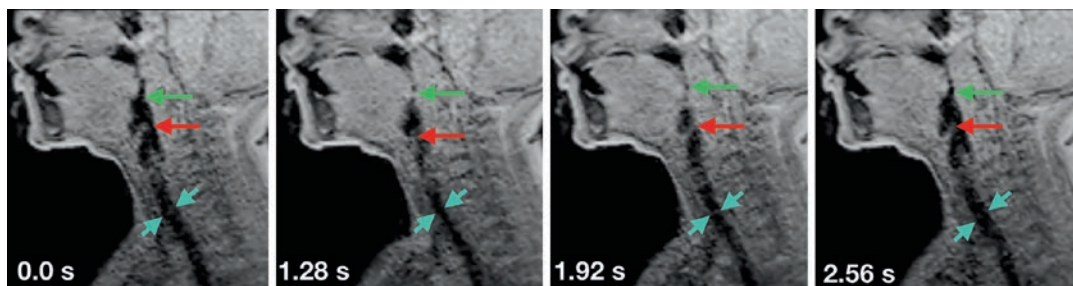


Fig. 13.7 3D cine MRI of obstructive sleep apnea. Midline sagittal slices through a 3D cine (or 4D) MRI image of an 11-year-old male patient with obstructive sleep apnea (OSA). A 3D image is captured every 0.32 s, and a panel is shown for four images throughout a breath. The motion of the airway as the patient breathes freely

under sedation is indicated by the arrows. Red arrows indicate the motion of the epiglottis, green arrows show the different positions of the soft palate, and blue arrows show the changing patency of the trachea. (Courtesy of Alister Bates, PhD, at Cincinnati Children's Hospital)

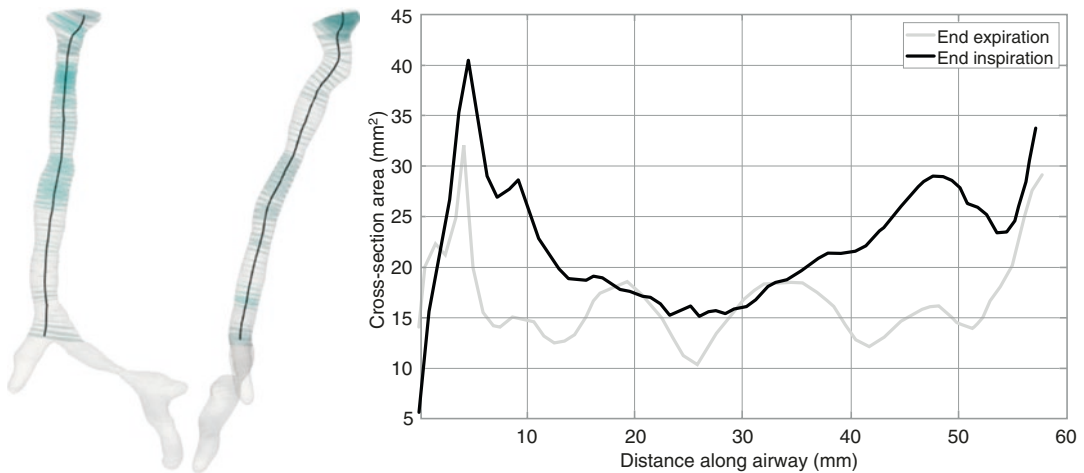


Fig. 13.8 Airway lumen measurements. Left: Coronal and sagittal views of an airway surface derived from a segmentation of ultrashort echo-time (UTE) MRI of a neonate with bronchopulmonary dysplasia. The airway surface is shown in gray, the airway centerline is shown in black, and disks representing the airway lumen 90° to the centerline are shown in blue at 1 mm intervals. Right:

Measuring the cross-sectional area of these luminal disks along the length of the airway produces a map of airway area. Repeating these measurements during different phases of breathing demonstrates the dynamics of the airway through breathing (airway area at end-inspiration and end-expiration in black and gray, respectively). (Courtesy of Alister Bates, PhD, at Cincinnati Children's Hospital)

achieve by viewing imaging slices alone because the airway curves from the nasal and oral airways into the pharynx and the descending airway may not be aligned with the axes of the images. Images can be reformatted to create off-axes images, although this can be time consuming to perform along the entire airway, and the airway may not maintain the same axis along its entire length. An alternative approach involves creating a virtual airway surface via segmentation or edge detection of the airway wall from high-resolution images. A centerline can be produced following the path of the airway, as is often done in analysis of vasculature [58]. The airway can then be assessed relative to its centerline, instead of an arbitrary imaging plane, producing a true cross-sectional area, which is invariant to the position of the patient in the scanner and airway curvature (Fig. 13.8) [57, 59, 60].

Using these techniques, it has been demonstrated that airway curvature may play as significant a role as airway constriction in contributing to patient symptoms, despite current clinical guidelines only considering the latter [57, 59]. Repeating these measurements on the 4D imaging techniques used above allows analysis of how

the airway size and shape change during a breath in dynamic conditions such as OSA and TM. For example, in neonatal TM, the ratio of the major and minor diameters has been found to be a strong indicator of tracheomalacia [52]. CT of patients with COPD revealed modest correlation between the area of the fourth and fifth tracheal branches and FEV₁ measurements [61].

Calculating Airway Function: Computational Fluid Dynamics

Both bronchoscopy and the imaging analysis techniques described in this chapter are visual or geometric assessments of the airway. These techniques reveal the size and shape of the airway but cannot reveal how these factors influence airflow. In cardiovascular medicine, several techniques have been developed to analyze blood flow through its velocity (measured via phase contrast MRI) and pressures (measured via cardiac catheterization). These imaging techniques cannot directly image the inhaled air since the flowing medium lacks sufficient density, but similar aerodynamic measures can be revealed by computa-

tional simulations of airflow known as computational fluid dynamics (CFD).

CFD can reveal the behavior of air as it is inhaled and exhaled via calculating the physics equation governing airflow (the Navier-Stokes equations). It can calculate the breathing effort used to move air in and out of the lungs, the pressures generated in moving the air, the forces that air pressure applies to the airway wall, and the transport of heat, water vapor, and inhaled toxic or therapeutic particles. This information can be used by clinicians to:

1. Determine the contribution of airway abnormalities to patient symptoms. For example, in a patient with both lung and airway complications (such as infants with bronchopulmonary dysplasia, BPD), CFD can reveal the extra effort needed to breathe due to just the airway abnormality [57].
2. Identify sites causing elevated airway resistance [62]. In OSA, it is common for patients to have multilevel obstruction. Using CFD, the local resistance at each of these locations can be mapped, and the cause of collapse at each location determined. This analysis can aid surgical planning by identifying the sites at which surgical interventions will cause the most benefit. This may not be apparent from imaging alone, as resistance in one region of the airway may cause collapse in an entirely different region.
3. Identify the causes of airway motion. For example, in OSA, some airway collapse is caused by low air pressure pulling the walls inwards (passive collapse), and other motion is caused by neuromuscular control [55, 56, 63, 64]. These two different types of motion may require different treatment strategies.
4. Particle inhalation can reveal deposition maps for inhaled therapeutic drugs; this can be used to determine the size and amount of particles necessary to obtain a certain dosage at a particular level of the airway [65–67].

An example of the clinical use of CFD was in the assessment of airway function in the first pediatric patient with a decellularized cadaveric transplanted trachea. The transplanted airway

segment did not grow as rapidly as the host tracheal segments, leading to an hour-glass-shaped trachea. CFD revealed that the patient's breathing effort had doubled in the 4 years following the transplantation [62].

Although CFD offers the potential to provide clinically significant information, it requires accurate physiological and anatomic data in order to provide meaningful results. Historically, the computational power required for accurate simulations was prohibitive; so, many simulations were based on simplifications from real physiology and anatomy. For example, simple idealized airway geometries were used, steady flow rates were considered rather than reciprocating inhalation and exhalation, and airflow turbulence was greatly simplified or ignored. As computational power has increased, CFD simulations are now capable of closely replicating *in vivo* conditions. To perform accurate CFD, a virtual airway surface must be created that accurately follows the shape of the real airway. This is obtained by segmenting images of the airway, historically from CT, but new techniques for nonionizing, high-resolution 3D MRI can also now be used (such as UTE MRI; see above), providing the potential for serial studies of disease development and treatment efficacy. The accuracy of the airway segmentation can affect the results of the CFD simulation, with measures such as pressure drop, and airway resistance being particularly sensitive to changes in airway segmentation parameters. One study found that changing the CT image segmentation threshold from -800 to -300 Hounsfield Units changed the calculated unilateral nasal resistance by 52% [68]. The phase of breathing and breathing maneuver during which imaging is obtained must be considered, as the airway shape may be significantly different during a breath hold compared to vigorous inhalation and likewise between a breath-hold and free-breathing. Such differences in airway shape may significantly alter findings from the CFD simulation. The location and extent of the airway coverage must also be considered. Airflow is affected by the flow upstream and downstream of any point of interest; therefore, if nasal airflow is of interest, the exterior face (where flow devel-

ops) must be included in the virtual model [69], and if tracheal airflow is of interest, then the glottis must be included [70, 71]. In addition to an accurate virtual airway surface, accurate breathing flow-rate information must be provided to the model, and this can be obtained through a pneumotach worn by the patient during breathing, hot-wire anemometry, or by analyzing the change in lung volume [55, 56, 72, 73].

When considering airway conditions that involve significant motion, such as OSA or tracheomalacia, this motion should be incorporated into the CFD model (Fig. 13.9) [74]. Two techniques have been proposed: fluid structure interaction (FSI) and using prescribed wall motion obtained from dynamic imaging. FSI techniques model motion by calculating the deformation of the structures surrounding the airway based on their material properties, but to date, FSI simulations have incorporated only passive airway

motion [74–79]. However, in OSA, synchronous imaging and breathing measurements have shown that there is a significant degree of neuromuscular control governing airway collapse in addition to passive motion [63, 64]. The second approach, which incorporates real airway wall motion from dynamic images via image registration and prescribing this motion to the virtual airway wall allows all forms of airway wall motion to be incorporated into the CFD simulation (Fig. 13.9) [55, 56].

Finally, airflow must be modeled appropriately. During restful breathing, airflow may be laminar in the nose, turbulent in the subglottic region, and transitional elsewhere in the central airways [65, 67, 80, 81]. Flow may be modelled as steady (not changing with time), quasi-steady (allowing the internal flow to change with time, but the airflow rate is constant) or fully unsteady (as in a realistic breath). While the most realistic

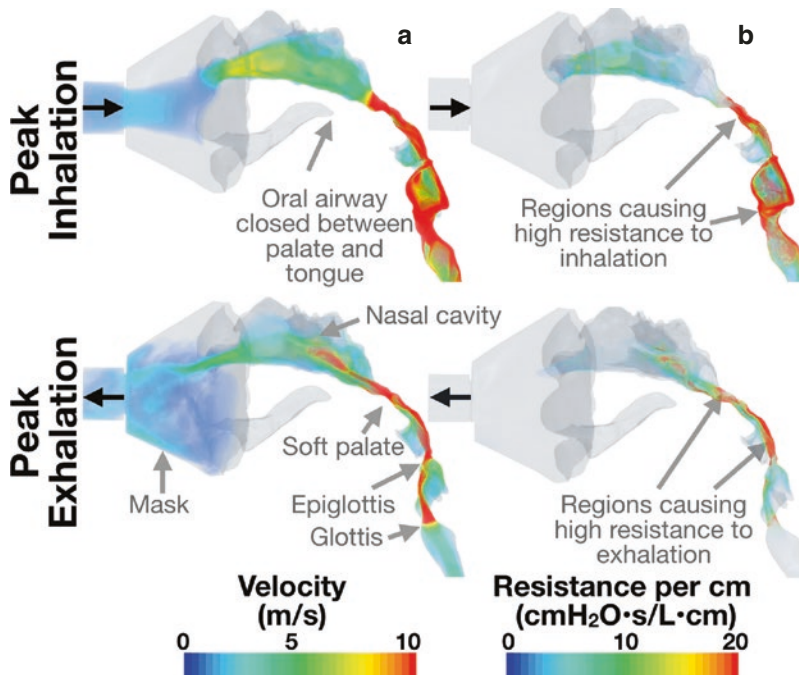


Fig. 13.9 CFD simulations. Computational fluid dynamics (CFD) simulation results in an 11-year-old patient with OSA. (a) Simulation results for airflow velocity at peak inhalation (upper) and peak exhalation (lower). The formation of high-speed jets can be seen in the oropharynx and after constrictions as the airflow navigates the

epiglottis and glottis. (b) The resistance to airflow per centimeter of the airflow traversed. Regions of high resistance are highlighted in the retropalatal airway and hypopharynx. (Courtesy of Alister Bates, PhD, at Cincinnati Children's Hospital)

computational model would allow for fully turbulent, unsteady airflow, this may come at a high computational cost. As with the other simplifications and assumptions that can be made in CFD simulations, quicker approaches that provide the necessary clinical information may be adopted in preference to more realistic simulations that take much more time or computing power [80, 82].

Limitations of Image-Based Airway Assessment

All imaging techniques are sensitive to the position in which the patient is imaged and the phase of breathing during which images were obtained. Head position can change the interpretation of medical imaging and is sensitive to rotation and flexion in particular. A major disadvantage of imaging is that the position of the patient cannot be changed as easily as during bronchoscopy, where maneuvers such as jaw thrust may be performed to gain an impression of the airway in different positions. In pediatrics, maintaining the correct position for the duration of imaging may be particularly challenging, and immobilization devices or sedation may be necessary in children below 4 years of age [26].

The different modalities discussed in this chapter also use various techniques to control the phase of breathing in which imaging is obtained, but standard techniques do not capture the airway's behavior throughout natural breathing or through breathing maneuvers that may be induced during bronchoscopy, such as a cough.

Summary

Radiological evaluations of central airway abnormalities in pediatrics can provide novel information that is unique and beyond that acquired through bronchoscopic assessment. Current clinical practice frequently utilizes imaging modalities such as X-ray radiograph, CT, or MRI to noninvasively detect and assess static and dynamic airway conditions. Emerging techniques have obviated some of the challenges of current imaging methods related

to patient safety and natural breathing conditions, particularly in MRI, and also can yield functional information related to abnormal airflow, such as with CFD simulations. These CFD simulations can quantify factors such as breathing effort, pressure losses, the forces acting on the airway walls, and inhaled particle depositions. With a high level of safety and repeatability, modern imaging methods allow for serial monitoring of disease progression and response to therapeutic and/or surgical treatment. Non-bronchoscopic tomographic imaging of the central airway has the potential to play a pivotal role in quantitatively assessing a wide range of pediatric airway conditions and in refining our understanding of how airway anatomy, motion, and airflow affect an individual patient's ventilation and work of breathing.

References

1. Hysinger E, Friedman N, Jensen E, Zhang H, Piccione J. Bronchoscopy in neonates with severe bronchopulmonary dysplasia in the NICU. *J Perinatol* [Internet]. Nature Publishing Group; 2019 [cited 2019 Feb 19];39(2):263–8. Available from: <http://www.nature.com/articles/s41372-018-0280-y>.
2. Burg G, Hysinger E, Hossain M, Wood R. Evaluation of agreement on presence and severity of tracheobronchomalacia in pediatric patients by dynamic flexible bronchoscopy. In: *Proceedings of the American Thoracic Society*.
3. Stagnaro N, Rizzo F, Torre M, Cittadini G, Magnano G. Multimodality imaging of pediatric airways disease: indication and technique. *Radiol Med* [Internet]. Springer Milan; 2017 [cited 2019 Feb 19];122(6):419–29. Available from: <http://link.springer.com/10.1007/s11547-017-0737-7>.
4. Koshy T, Misra S, Chatterjee N, Dharan BS. Accuracy of a chest X-Ray-based method for predicting the depth of insertion of endotracheal tubes in pediatric patients undergoing cardiac surgery. *J Cardiothorac Vasc Anesth* [Internet]. W.B. Saunders; 2016 [cited 2019 Feb 19];30(4):947–53. Available from: <https://www.sciencedirect.com/science/article/pii/S105307701600063X>.
5. Lee EY, Restrepo R, Dillman JR, Ridge CA, Hammer MR, Boiselle PM. Imaging evaluation of pediatric trachea and bronchi: systematic review and updates. *Semin Roentgenol*. 2012;47(2):182–96.
6. Laya BF, Lee EY. Congenital causes of upper airway obstruction in pediatric patients: updated imaging techniques and review of imaging findings. *Semin Roentgenol* [Internet]. 2012 [cited 2019 Feb

- 19];47(2):147–58. Available from: <http://www.ncbi.nlm.nih.gov/pubmed/22370193>.
7. Chapman T, Sandstrom CK, Parnell SE. Pediatric emergencies of the upper and lower airway. *Appl Radiol*. 2012;41:10–7.
 8. Huang C-C, Shih S-L. Steeple sign of croup. *N Engl J Med*. 2012;367(1).
 9. George JR, Chung S, Nielsen I, Goldberg AN, Miller A, Kezirian EJ. Comparison of drug-induced sleep endoscopy and lateral cephalometry in obstructive sleep apnea. *Laryngoscope* [Internet]. John Wiley & Sons, Ltd; 2012 [cited 2019 Feb 1];122(11):2600–5. Available from: <http://doi.wiley.com/10.1002/lary.23561>.
 10. Lee EY, Greenberg SB, Boiselle PM. Multidetector computed tomography of pediatric large airway diseases: state-of-the-art. *Radiol Clin North Am* [Internet]. Elsevier; 2011 [cited 2019 Feb 8];49(5):869–93. Available from: <https://linkinghub.elsevier.com/retrieve/pii/S0033838911000765>.
 11. Lee EY. Advancing CT and MR imaging of the lungs and airways in children: imaging into practice. *Pediatr Radiol* [Internet]. Springer; 2008 [cited 2019 Feb 8];38(S2):208–12. Available from: <http://link.springer.com/10.1007/s00247-008-0767-3>.
 12. Lee EY, Siegel MJ. MDCT of tracheobronchial narrowing in pediatric patients. *J Thorac Imaging* [Internet]. 2007 [cited 2019 Feb 8];22(3):300–9. Available from: <https://insights.ovid.com/crossref?an=00005382-200708000-00020>.
 13. Sanal B, Demirhan N, Koplay M, Sadikoğlu MY, Gürpınar A. Congenital nasal piriform aperture stenosis: clinical and radiologic findings and treatment. *Jpn J Radiol*. 2009;27(9):389–91.
 14. Belden CJ, Mancuso AA, Schmalfluss IM. CT features of congenital nasal piriform aperture stenosis: initial experience. *Radiology*. 2013.
 15. Rachmiel A, Emodi O, Aizenbud D. Management of obstructive sleep apnea in pediatric craniofacial anomalies. *Ann Maxillofac Surg* [Internet]. Wolters Kluwer – Medknow Publications; 2012 [cited 2019 Feb 1];2(2):111–5. Available from: <http://www.ncbi.nlm.nih.gov/pubmed/23483041>.
 16. Slaats MA, Van Hoorenbeeck K, Van Eyck A, Vos WG, De Backer JW, Boudewyns A, et al. Upper airway imaging in pediatric obstructive sleep apnea syndrome. *Sleep Med Rev* [Internet]. W.B. Saunders; 2015 [cited 2019 Feb 1];21:59–71. Available from: <https://www.sciencedirect.com/science/article/pii/S1087079214000823>.
 17. Abramson Z, Susarla SM, Lawler M, Bouchard C, Troulis M, Kaban LB. Three-dimensional computed tomographic airway analysis of patients with obstructive sleep apnea treated by maxillomandibular advancement. *J Oral Maxillofac Surg* [Internet]. W.B. Saunders; 2011 [cited 2019 Feb 1];69(3):677–86. Available from: <https://www.sciencedirect.com/science/article/pii/S0278239110016150>.
 18. Li H-Y, Lo Y-L, Wang C-J, Hsin L-J, Lin W-N, Fang T-J, et al. Dynamic drug-induced sleep computed tomography in adults with obstructive sleep apnea. *Sci Rep* [Internet]. Nature Publishing Group; 2016 [cited 2019 Feb 1];6(1):35849. Available from: <http://www.nature.com/articles/srep35849>.
 19. Vos WG, De Backer WA, Verhulst SL. Correlation between the severity of sleep apnea and upper airway morphology in pediatric and adult patients. *Curr Opin Allergy Clin Immunol* [Internet]. 2010 [cited 2017 Feb 6];10(1):26–33. Available from: <http://content.wkhealth.com/linkback/openurl?sid=WKPTLP:landi ngpage&an=00130832-201002000-00006>.
 20. Zhang P, Ye J, Pan C, Xian J, Sun N, Li J, et al. Comparison of drug-induced sleep endoscopy and upper airway computed tomography in obstructive sleep apnea patients. *Eur Arch Oto-Rhino-Laryngology* [Internet]. 2014 [cited 2019 Feb 1];271(10):2751–6. Available from: <http://link.springer.com/10.1007/s00405-014-3051-1>.
 21. McDaniel LS, Poynot WJ, Gonthier KA, Dunham ME, Crosby and TW. Image-based 3-dimensional characterization of laryngotracheal stenosis in children. *OTO Open* [Internet]. SAGE Publications, Sage CA: Los Angeles, CA; 2018 [cited 2019 Feb 19];2(1):2473974X1775358. Available from: <http://journals.sagepub.com/doi/10.1177/2473974X17753583>.
 22. Lee EY, Tracy DA, Bastos M d’Almeida, Casey AM, Zurakowski D, Boiselle PM. Expiratory volumetric MDCT evaluation of air trapping in pediatric patients with and without tracheomalacia. *Am J Roentgenol* [Internet]. American Roentgen Ray Society; 2010 [cited 2019 Feb 4];194(5):1210–5. Available from: <http://www.ajronline.org/doi/10.2214/AJR.09.3259>.
 23. Pearce MS, Salotti JA, Little MP, McHugh K, Lee C, Kim KP, et al. Radiation exposure from CT scans in childhood and subsequent risk of leukaemia and brain tumours: A retrospective cohort study. *Lancet* [Internet]. 2012 [cited 2018 Sep 14];380(9840):499–505. Available from: <http://www.ncbi.nlm.nih.gov/pubmed/22681860>.
 24. Singh S, Kalra MK, Moore MA, Shailam R, Liu B, Toth TL, et al. Dose reduction and compliance with pediatric CT protocols adapted to patient size, clinical indication, and number of prior studies. *Radiology*. 2009;252(1):200–8.
 25. Yu H, Zhao S, Hoffman EA, Wang G. Ultra-low dose lung CT perfusion regularized by a previous scan. *Acad Radiol*. 2009;16(3):363–73.
 26. Lee E. *Pediatric radiology: practical imaging evaluation of infants and children*. Lippincott Williams & Wilkins; 2017.
 27. Lustig M, Donoho D, Pauly JM. Sparse MRI: the application of compressed sensing for rapid MR imaging. *Magn Reson Med* [Internet]. John Wiley & Sons, Ltd; 2007 [cited 2019 Feb 19];58(6):1182–95. Available from: <http://doi.wiley.com/10.1002/mrm.21391>.
 28. Higano NS, Hahn AD, Tkach JA, Cao X, Walkup LL, Thomen RP, et al. Retrospective respiratory self-gating and removal of bulk motion in pulmonary

- UTE MRI of neonates and adults. *Magn Reson Med*. 2017;77(3):1284–95.
29. Fleck RJ, Shott SR, Mahmoud M, Ishman SL, Amin RS, Donnelly LF. Magnetic resonance imaging of obstructive sleep apnea in children. *Pediatr Radiol* [Internet]. 2018 [cited 2018 Sep 14];48(9):1223–33. Available from: <http://www.ncbi.nlm.nih.gov/pubmed/30078047>.
 30. Nayak KS, Fleck RJ. Seeing Sleep: Dynamic imaging of upper airway collapse and collapsibility in children. *IEEE Pulse* [Internet]. 2014 [cited 2019 Feb 19];5(5):40–4. Available from: <http://ieeexplore.ieee.org/document/6908108/>.
 31. Manickam PV, Shott SR, Boss EF, Cohen AP, Meinen-Derr JK, Amin RS, et al. Systematic review of site of obstruction identification and non-CPAP treatment options for children with persistent pediatric obstructive sleep apnea. *Laryngoscope* [Internet]. Wiley-Blackwell; 2016 [cited 2018 Sep 13];126(2):491–500. Available from: <http://doi.wiley.com/10.1002/lary.25459>.
 32. Shott SR, Donnelly LF. Cine magnetic resonance imaging: evaluation of persistent airway obstruction after tonsil and adenoidectomy in children with Down syndrome. *Laryngoscope* [Internet]. John Wiley & Sons, Inc.; 2004 [cited 2017 Mar 28];114(10):1724–9. Available from: <http://www.ncbi.nlm.nih.gov/pubmed/15454761>.
 33. Kundra P, Mishra SK, Ramesh A. Ultrasound of the airway. *Indian J Anaesth*. 2011;55(5):456.
 34. Šuštić A, Kovač D, Žgaljardić Z, Župan Ž, Krstulović B. Ultrasound-guided percutaneous dilatational tracheostomy: a safe method to avoid cranial misplacement of the tracheostomy tube. *Intensive Care Med*. 2000;26(9):1379–81.
 35. Hatfield A, Bodenham A. Portable ultrasonic scanning of the anterior neck before percutaneous dilatational tracheostomy. *Anaesthesia*. 1999;54(7):660–3.
 36. Vats A, Worley GA, de Bruyn R, Porter H, Albert DM, Bailey CM. Laryngeal ultrasound to assess vocal fold paralysis in children. *J Laryngol Otol* [Internet]. 2004 [cited 2019 Feb 27];118(06):429–31. Available from: <http://www.ncbi.nlm.nih.gov/pubmed/15285860>.
 37. Rossler L, Rothoefl T, Teig N, Koerner-Rettberg C, Deitmer T, Rieger CHL, et al. Ultrasound and colour Doppler in infantile subglottic haemangioma. *Pediatr Radiol* [Internet]. Springer-Verlag; 2011 [cited 2019 Feb 27];41(11):1421–8. Available from: <http://link.springer.com/10.1007/s00247-011-2213-1>.
 38. Ko DR, Chung YE, Park I, Lee H-J, Park JW, You JS, et al. Use of bedside sonography for diagnosing acute epiglottitis in the emergency department. *J Ultrasound Med* [Internet]. John Wiley & Sons, Ltd; 2012 [cited 2019 Feb 27];31(1):19–22. Available from: <http://doi.wiley.com/10.7863/jum.2012.31.1.19>.
 39. Lakhal K, Delplace X, Cottier JP, Tranquart F, Sauvagnac X, Mercier C, et al. The feasibility of ultrasound to assess subglottic diameter. *Anesth Analg*. 2007;104(3):611–4.
 40. Singh M, Chin KJ, Chan VWS, Wong DT, Prasad GA, Yu E. Use of sonography for airway assessment: an observational study. *J Ultrasound Med*. 2010;29(1):79–85.
 41. Gibson SE, Strife JL, Myer CM, O'Connor DM. Sleep fluoroscopy for localization of upper airway obstruction in children. *Ann Otol Rhinol Laryngol* [Internet]. SAGE Publications, Sage CA: Los Angeles, CA; 1996 [cited 2019 Feb 19];105(9):678–83. Available from: <http://journals.sagepub.com/doi/10.1177/000348949610500902>.
 42. Goding GS, Tesfayesus W, Kezirian EJ. Hypoglossal nerve stimulation and airway changes under fluoroscopy. *Otolaryngol Head Neck Surg*. 2012;146(6):1017–22.
 43. Isaiah A, Pereira KD. Laryngotracheal anomalies and airway fluoroscopy in infants. *Int J Pediatr Otorhinolaryngol* [Internet]. Elsevier; 2017 [cited 2019 Feb 19];97:109–12. Available from: <https://www.sciencedirect.com/science/article/pii/S0165587617301337>.
 44. Teh BM, Hall C, Kleid S. Infected tracheocele (acquired tracheal diverticulum): case report and literature review. *J Laryngol Otol*. 2011;125(5):540.
 45. Sharma BG. Tracheal diverticulum: a report of 4 cases. *Ear Nose Throat J*. 2009;88(1):E11.
 46. Soto-Hurtado EJ, Peñuela-Ruiz L, Rivera-Sánchez I, Torres-Jiménez J. Tracheal diverticulum: a review of the literature. *Lung*. 2006;184(6):303–7.
 47. Su SC, Masters IB, Buntain H, Frawley K, Sarikwal A, Watson D, et al. A comparison of virtual bronchoscopy versus flexible bronchoscopy in the diagnosis of tracheobronchomalacia in children. *Pediatr Pulmonol*. 2017;52(4):480–6.
 48. Hatabu H, Alsop DC, Listerud J, Bonnet M, Geffer WB. T2* and proton density measurement of normal human lung parenchyma using submillisecond echo time gradient echo magnetic resonance imaging. *Eur J Radiol*. 1999;29(3):245–52.
 49. Johnson KM, Fain SB, Schiebler ML, Nagle S. Optimized 3D ultrashort echo time pulmonary MRI. *Magn Reson Med*. 2013;70(5):1241–50.
 50. Lederlin M, Crémillieux Y. Three-dimensional assessment of lung tissue density using a clinical ultrashort echo time at 3 tesla: a feasibility study in healthy subjects. *J Magn Reson Imaging*. 2013;40(4):839–47.
 51. Dournes G, Grodzki D, Macey J, Girodet P-O, Fayon M, Chateil J-F, et al. Quiet submillimeter MR imaging of the lung is feasible with a PETRA sequence at 1.5 T. *Radiology*. 2015;276(1):258–65.
 52. Bates AJ, Higano NS, Hysinger EB, Fleck RJ, Hahn AD, Fain SB, et al. Quantitative assessment of regional dynamic airway collapse in neonates via retrospectively respiratory-gated ¹H ultrashort echo time MRI. *J Magn Reson Imaging* [Internet]. Wiley-Blackwell; 2018 [cited 2018 Sep 26]; Available from: <http://doi.wiley.com/10.1002/jmri.26296>.
 53. Higano NS, Bates AJ, Tkach JA, Fleck RJ, Lim FY, Woods JC, et al. Pre- and post-operative visualization of neonatal esophageal atresia/tracheoesophageal fis-

- tula via magnetic resonance imaging. *J Pediatr Surg Case Rep* [Internet]. 2018 [cited 2017 Oct 9];29:5–8. Available from: <http://www.ncbi.nlm.nih.gov/pubmed/29399473>.
54. Wu Z, Chen W, Khoo MCK, Davidson Ward SL, Nayak KS. Evaluation of upper airway collapsibility using real-time MRI. *J Magn Reson Imaging*. 2016;44(1):158–67.
 55. Bates AJ, Schuh A, Amine-Eddine G, McConnell K, Loew W, Fleck RJ, et al. Assessing the relationship between movement and airflow in the upper airway using computational fluid dynamics with motion determined from magnetic resonance imaging. *Clin Biomech* [Internet]. Elsevier; 2017 [cited 2017 Oct 24];0(0). Available from: <http://linkinghub.elsevier.com/retrieve/pii/S0268003317302231>.
 56. Bates AJ, Schuh A, McConnell K, Williams BM, Lanier JM, Willmering MM, et al. A novel method to generate dynamic boundary conditions for airway CFD by mapping upper airway movement with non-rigid registration of dynamic and static MRI. *Int j numer method biomed eng* [Internet]. Wiley-Blackwell; 2018 [cited 2018 Sep 4];e3144. Available from: <http://doi.wiley.com/10.1002/cnm.3144>.
 57. Bates AJ, Cetto R, Doorly DJ, Schroter RC, Tolley NS, Comerford A. The effects of curvature and constriction on airflow and energy loss in pathological tracheas. *Respir Physiol Neurobiol*. 2016;234:69–78.
 58. Piccinelli M, Veneziani A, Steinman DA, Remuzzi A, Antiga L. A framework for geometric analysis of vascular structures: application to cerebral aneurysms. *IEEE Trans Med Imaging IEEE*. 2009;28(8):1141–55.
 59. Bates AJ, Comerford A, Cetto R, Schroter RC, Tolley NS, Doorly DJ. Power loss mechanisms in pathological tracheas. *J Biomech* [Internet]. Elsevier; 2016 [cited 2016 May 13];49(11):2187–92. Available from: <http://linkinghub.elsevier.com/retrieve/pii/S0021929015006752>.
 60. Tschirren J, Hoffman EA, McLennan G, Sonka M. Intrathoracic airway trees: segmentation and airway morphology analysis from low-dose CT scans. *IEEE Trans Med Imaging*. 2005;24(12):1529–39.
 61. Schroeder JD, McKenzie AS, Zach JA, Wilson CG, Curran-Everett D, Stinson DS, et al. Relationships between airflow obstruction and quantitative CT measurements of emphysema, air trapping, and airways in subjects with and without chronic obstructive pulmonary disease. *Am J Roentgenol* [Internet]. American Roentgen Ray Society; 2013 [cited 2019 Feb 28];201(3):W460–70. Available from: <http://www.ajronline.org/doi/10.2214/AJR.12.10102>.
 62. Hamilton NJ, Kanani M, Roebuck DJ, Hewitt RJ, Cetto R, Culme-Seymour EJ, et al. Tissue-engineered tracheal replacement in a child: a 4-year follow-up study. *Am J Transplant* [Internet]. Wiley Online Library; 2015;15(10):2750–7. Available from: <http://doi.wiley.com/10.1111/ajt.13318>.
 63. Schwab RJ, Gefter WB, Hoffman EA, Gupta KB, Pack AI. Dynamic upper airway imaging during awake respiration in normal subjects and patients with sleep disordered breathing. *Am Rev Respir Dis* [Internet]. American Lung Association; 1993 [cited 2016 May 26];148(5):1385–400. Available from: <http://www.atsjournals.org/doi/abs/10.1164/ajrccm/148.5.1385>.
 64. Schwab RJ, Gefter WB, Pack AI, Hoffman EA. Dynamic imaging of the upper airway during respiration in normal subjects. *J Appl Physiol*. 1993;74(4):1504–14.
 65. Calmet H, Houzeaux G, Vázquez M, Eguzkitza B, Gambaruto AM, Bates AJ, et al. Flow features and micro-particle deposition in a human respiratory system during sniffing. *J Aerosol Sci* [Internet]. 2018 [cited 2018 May 29]; Available from: <http://linkinghub.elsevier.com/retrieve/pii/S0021850218300375>.
 66. Calmet H, Kleinstreuer C, Houzeaux G, Kolanjiyl A V., Lehmkühl O, Olivares E, et al. Subject-variability effects on micron particle deposition in human nasal cavities. *J Aerosol Sci* [Internet]. Pergamon; 2017 [cited 2017 Oct 24]; Available from: <https://www.sciencedirect.com/science/article/pii/S0021850217301933>.
 67. Calmet H, Gambaruto AM, Bates AJ, Vázquez M, Houzeaux G, Doorly DJ. Large-scale CFD simulations of the transitional and turbulent regime for the large human airways during rapid inhalation. *Comput Biol Med*. 2016;69:166–80.
 68. Cherobin GB, Voegels RL, Gebrim EMMS, Garcia GJM. Sensitivity of nasal airflow variables computed via computational fluid dynamics to the computed tomography segmentation threshold. 2018 [cited 2019 Jan 16]; Available from: <https://doi.org/10.1371/journal.pone.0207178.t001>.
 69. Taylor DJ, Doorly DJ, Schroter RC. Inflow boundary profile prescription for numerical simulation of nasal airflow. *J R Soc Interface* [Internet]. 2010;7(44):515–27. Available from: <http://rsif.royalsocietypublishing.org/cgi/doi/10.1098/rsif.2009.0306>.
 70. Lin CL, Tawhai MH, McLennan G, Hoffman EA. Characteristics of the turbulent laryngeal jet and its effect on airflow in the human intrathoracic airways. *Respir Physiol Neurobiol Elsevier*. 2007;157(2–3):295–309.
 71. Collier GJ, Kim M, Chung Y, Wild JM. 3D phase contrast MRI in models of human airways: Validation of computational fluid dynamics simulations of steady inspiratory flow. *J Magn Reson Imaging* [Internet]. 2018 [cited 2018 Oct 16]; Available from: <http://www.ncbi.nlm.nih.gov/pubmed/29630757>.
 72. Rennie CE, Gouder KA, Taylor DJ, Tolley NS, Schroter RC, Doorly DJ. Nasal inspiratory flow: at rest and sniffing. *Int Forum Allergy Rhinol*. 2011;1(2):128–35.
 73. Miyawaki S, Choi S, Hoffman EA, Lin CL. A 4DCT imaging-based breathing lung model with relative hysteresis. *J Comput Phys* [Internet]. Elsevier Inc.; 2016;326:76–90. Available from: <https://doi.org/10.1016/j.jcp.2016.08.039>.
 74. Zhao M, Barber T, Cistulli PA, Sutherland K, Rosengarten G. Simulation of upper airway occlusion without and with mandibular advancement

- in obstructive sleep apnea using fluid-structure interaction. *J Biomech* [Internet]. 2013 [cited 2016 May 26];46(15):2586–92. Available from: <http://www.sciencedirect.com/science/article/pii/S0021929013003904>.
75. Wang Y, Wang J, Liu Y, Yu S, Sun X, Li S, et al. Fluid-structure interaction modeling of upper airways before and after nasal surgery for obstructive sleep apnea. *Int j numer method biomech eng* [Internet]. John Wiley & Sons, Ltd; 2012 [cited 2017 Mar 3];28(5):528–46. Available from: <http://doi.wiley.com/10.1002/cnm.1486>.
76. Zhu JH, Lee HP, Lim KM, Lee SJ, Teo LSL, Wang DY. Passive movement of human soft palate during respiration: A simulation of 3D fluid/structure interaction. *J Biomech* [Internet]. 2012 [cited 2017 Mar 3];45(11):1992–2000. Available from: <http://linkinghub.elsevier.com/retrieve/pii/S0021929012002734>.
77. Pirnar J, Dolenc-Grošelj L, Fajdiga I, Žun I. Computational fluid-structure interaction simulation of airflow in the human upper airway. *J Biomech* [Internet]. 2015 [cited 2017 Mar 3];48(13):3685–91. Available from: <http://linkinghub.elsevier.com/retrieve/pii/S002192901500456X>.
78. Ashaat S, Al-Jumaily AM. Reducing upper airway collapse at lower continuous positive airway titration pressure. *J Biomech* [Internet]. 2016 [cited 2017 Mar 3];49(16):3915–22. Available from: <http://linkinghub.elsevier.com/retrieve/pii/S0021929016311630>.
79. Zhao M, Barber T, Cistulli P, Sutherland K, Rosengarten G. Predicting the treatment response of oral appliances for obstructive sleep apnea using computational fluid dynamics and fluid-structure interaction simulations. In: Volume 3A: Biomedical and biotechnology engineering [Internet]. 2013. p. V03AT03A051. Available from: <http://proceedings.asmedigitalcollection.asme.org/proceeding.aspx?doi=10.1115/IMECE2013-62904>.
80. Bates AJ, Doorly DJ, Cetto R, Calmet H, Gambaruto AM, Tolley NS, et al. Dynamics of airflow in a short inhalation. *J R Soc Interface* [Internet]. 2014 [cited 2015 Aug 12];12(102):20140880. Available from: <http://rsif.royalsocietypublishing.org/cgi/doi/10.1098/rsif.2014.0880>.
81. Zhao K, Dalton P, Yang GC, Scherer PW, Chemical M, Hall H, et al. Numerical modeling of turbulent and laminar air ow and odorant transport during Sniffing in the human and rat nose. *Chem Senses*. 2006;31(2):107–18.
82. Bates AJ, Comerford A, Cetto R, Doorly DJ, Schroter RC, Tolley NS. Computational fluid dynamics benchmark dataset of airflow in tracheas. *Data Br* [Internet]. Elsevier; 2017 [cited 2017 Feb 24];10:101–7. Available from: <http://www.ncbi.nlm.nih.gov/pubmed/27981200>.